Biological and Environmental Controls on Evaporative Fractions at AmeriFlux Sites

CHUNLÜE ZHOU AND KAICUN WANG

State Key Laboratory of Earth Surface Processes and Resource Ecology, College of Global Change and Earth System Science, Beijing Normal University, and Joint Center for Global Change Studies, Beijing, China

(Manuscript received 7 May 2015, in final form 30 August 2015)

ABSTRACT

Knowledge of the evaporative fraction (EF: the ratio of latent heat flux to the sum of sensible and latent heat fluxes) and its controls is particularly important for accurate estimates of water flux, heat exchange, and ecosystem response to climatic changes. In this study, the biological and environmental controls on monthly EF were evaluated across 81 AmeriFlux sites, mainly in North America, for 2000–12. The land-cover types of these sites include forest, shrubland, grassland, and cropland, and the local climates vary from humid to arid. The results show that vegetation coverage, indicated by the normalized difference vegetation index (NDVI), has the best agreement with EF (site-averaged partial correlation coefficient $\rho = 0.53$; significance level $p < 0.05$) because of vegetation transpiration demand. The minimum air temperature is closely related to EF (site-averaged $\rho = 0.51$; $p < 0.05$) because of the inhibition of respiratory enzyme activity. Relative humidity, an indicator of surface aridity, shows a significant positive correlation with EF (site-averaged $\rho = 0.46$; $p < 0.05$). The impacts of wind speed and diurnal air temperature range on EF depend on land-cover types and are strong over grasslands and cropland. From these findings, empirical methods were established to predict monthly EF using meteorological data and NDVI. Correlation coefficients between EF estimates and observations range from 0.80 to 0.93, with root-mean-square errors varying from 0.09 to 0.12. This study demonstrates the varying controls on EF across different landscapes and enhances understanding of EF and its dynamics under changing climates.

1. Introduction

Evaporative fraction (EF) is the ratio of latent heat flux LE (in energy units of watts per meter squared) to the available energy (the difference between surface net radiation R_n and ground heat flux G) or to the sum of sensible heat flux H (also in energy units of watts per meter squared) and LE at the land surface, as shown in Eq. (1):

$$\mathrm{EF} = \frac{\mathrm{LE}}{R_n - G} = \frac{\mathrm{LE}}{\mathrm{LE} + H}. \tag{1}$$

Global circulation models, agricultural-management applications, and drought monitoring require estimates of LE and EF (Kustas and Anderson 2009; Shuttleworth 2007). Various empirically and physically based methods to estimate LE with different degrees of accuracy and complexity have been developed on the basis of either Monin–Obukhov similarity theory (MOST) or the Penman–Monteith equation (Wang and Dickinson 2012), typically with errors on the order of 15%–30% (Jiang et al. 2004; Kalma et al. 2008).

The Penman–Monteith equation has been recommended by the Food and Agriculture Organization of the United Nations as a standard method to calculate LE (Allen et al. 1998, pp. 17–28 and 65–77). The Penman–Monteith equation requires R_n and G, which are not measured routinely and are unavailable at regional or global scale, thus limiting its application. Furthermore, the Penman–Monteith equation needs canopy resistance r_c, which is difficult to measure directly (Wang and Dickinson 2012).

Therefore, many studies have tried to simplify the Penman–Monteith equation (Bailey et al. 1993; Kra 2010; Priestley and Taylor 1972; Rivas and Caselles 2004; Valiantzas 2006, 2013). One of the most widely used simplifications, the Priestley and Taylor equation,

Denotes Open Access content.

Corresponding author address: Dr. Kaicun Wang, State Key Laboratory of Earth Surface Processes and Resource Ecology, College of Global Change and Earth System Science, Beijing Normal University, Beijing, 100875, China.
E-mail: kcwang@bnu.edu.cn

DOI: 10.1175/JAMC-D-15-0126.1

can be used to calculate LE under adequate moisture conditions (Priestley and Taylor 1972). The Priestley and Taylor equation is not suitable for water-limited conditions, and it does not consider the impact of vegetation on LE either. In addition, the Priestley and Taylor equation does not fully consider the impact of atmospheric evaporative demand, that is, the impacts of wind speed (WS) and water vapor deficit.

Some remote sensing–based models to estimate LE are widely used (Mu et al. 2007a, 2011), but their disadvantages are obvious in terms of high sensitivity to errors of input data and limited availability in different conditions (Kalma et al. 2008; Teixeira et al. 2009a,b; Wang and Dickinson 2012). The use of satellite-derived surface temperature T_s for the aerodynamic temperature results in great uncertainty of surface flux estimates in one-source models, which has been questioned (Friedl 2002; Hall et al. 1992; Shuttleworth 1991). Two-source models require an unbiased gradient between T_s and surface air temperature T_a (Timmermans et al. 2007), but the uncertainty of T_s retrievals is several kelvin (Norman et al. 2000; Wang and Liang 2008). The T_s–vegetation space methods suffer from their key assumption that LE is negatively correlated with temperature (Wang et al. 2006). Therefore, some empirical models were proposed to estimate the global LE over different land-cover types. Take two cases as examples: 1) three suites of empirical models were proposed with routine meteorological observations including R_n, T_a, relative humidity (RH), diurnal temperature range (DTR), WS, and normalized difference vegetation index (NDVI) to obtain long-term series of LE (Wang et al. 2010, 2007; Wang and Liang 2008) and 2) the tree ensemble model was constructed with satellite remote sensing and surface meteorological observations to acquire the temporal variance and global spatial distribution of LE (Jung et al. 2009, 2010).

There are numerous published studies on LE for its connection of surface energy and water balance, but studies on EF and H are many fewer. As H heats air temperature above the surface, EF or H is more directly relevant for climatic-change study—for example, spatial warming contrast (Wang 2014; Wang and Zhou 2015). Even though some land-surface models are designed to provide EF or H, their accuracy is low (Best et al. 2015). Despite an accurate LE estimate, uncertainty of EF or H estimates through the energy-balance method is still large, particularly so when H dominates the available energy over dry regions and seasons.

Therefore, taking advantage of long-time measurements from 81 "AmeriFlux" sites, this study explored the biological and environmental controls on monthly EF for different ecosystems and types of climate. On the basis of the quantitative relationships between EF and its controls, empirical models were further established to estimate EF that can be widely used to estimate the long-term variance in EF from conventional weather observations. These will help in understanding the effect of land–atmosphere interactions on climatic change.

2. Data and methods

a. AmeriFlux data

The AmeriFlux network is a community of sites measuring ecosystem carbon, water, and energy fluxes across America for better understanding of terrestrial ecosystems in a changing world. The AmeriFlux network measures T_a, DTR, RH, WS, H, and LE at every 30 or 60 min over ~140 stations across a range of land-cover types (Baldocchi et al. 2001). These data are publicly available online (http://ameriflux.ornl.gov/). DTR quantifies the difference between the daily maximum and minimum air temperature. After quality control (see section 2b), a total of 81 sites with data spanning over 20 months were selected in this study. These sites (74 in America, 5 in Canada, and 2 in Brazil; Fig. 1) were divided into two groups that were each as well distributed as possible over all of the land-cover types: one group with 43 sites (Table 1) was used to parameterize EF, and the other group with 38 sites (Table 2) was used to validate the accuracy of the parameterizations. In this way, it makes the parameterizations of EF globally applicable. The data collected at all of the sites were used to investigate the biological and environmental controls on EF.

The flux data at study sites were measured by an eddy covariance (EC) system with the flux-tower height varying from 1.5 to 60 m above the ground surface. The elevation of the selected sites ranges from 1 to over 3000 m above sea level. The land-cover types include deciduous and evergreen forest, closed shrubland, grassland, cropland, and woody savanna (Tables 1 and 2). The climates vary from tropical and temperate to Mediterranean and from humid to arid.

b. Quality control of the AmeriFlux data

Before releasing the data, AmeriFlux implemented extensive quality control on them (Baldocchi et al. 2001); the data still contain outliers and erroneous records, and additional quality-control procedures were thus implemented. The additional quality control included the following procedures. 1) On the basis of historical records, H and LE values over 1600 $W\,m^{-2}$ or less than $-500\,W\,m^{-2}$ (Zahumenský 2004), T_a values outside the range from 56.67° to −62.22°C, DTR values exceeding 39.44°C, and WS values over 45 $m\,s^{-1}$ were

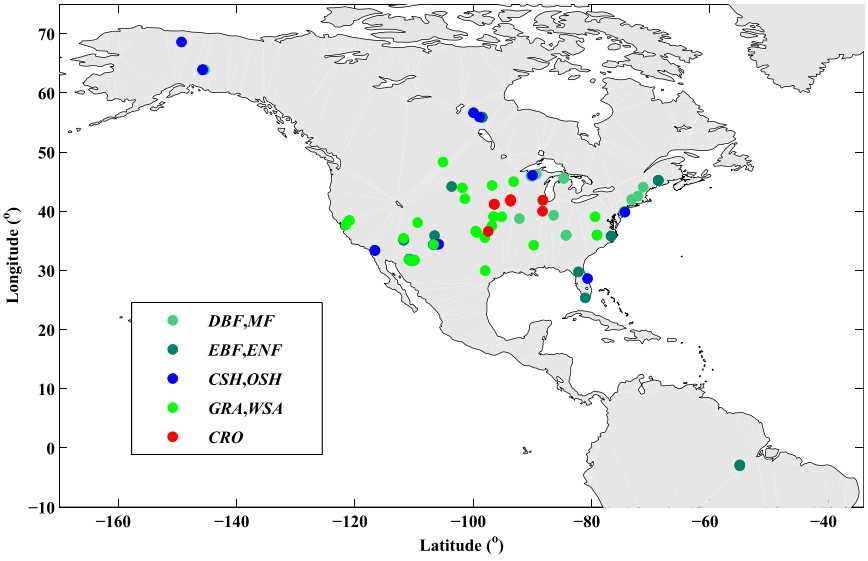

FIG. 1. Locations of the 81 AmeriFlux sites used in this study. These sites were divided into two groups for training and validating empirical methods to estimate EF; these groups were summarized in Tables 1 and 2, respectively. Light-green circles represent the 16 deciduous forest sites, dark-green circles represent the 17 evergreen forest sites, blue circles represent the 14 shrubland sites, green circles represent the 26 grassland sites, and red circles represent the 8 cropland sites. Land-cover types in the legend are deciduous broadleaf forest (DBF), mixed forest (MF), evergreen broadleaf forest (EBF), evergreen needleleaf forest (ENF), closed shrubland (CSH), open shrubland (OSH), grassland (GRA), woody savanna (WSA), and cropland (CRO).

excluded (Cerveny et al. 2007). 2) On the basis of physical characteristics, RH values outside the range 0%–100% were excluded. 3) Outliers beyond 5 standard deviations σ for all of the above variables were also excluded. Chebyshev's theorem demonstrates that this threshold results in more than 96% of the statistically acceptable data with any data distribution (Amidan et al. 2005; Schmidt et al. 2011).

After quality control, when both LE and H were available, other environmental variables were interpolated using a cubic method at points with adjacent gaps of less than 6 h. The most-interpolated variable is T_a with a ratio of 0.21% (the interpolated data length/the whole data length used in this study). It required the common record lengths of H, LE, T_a, NDVI, RH, and WS to be no less than 20 months. A total of 81 sites met the above requirements.

c. *MODIS VI products*

Three vegetation indices (VI) that quantify vegetation coverage are available from Moderate Resolution Imaging Spectroradiometer (MODIS) satellite land products after 2000 (http://modis.gsfc.nasa.gov/data/): leaf area index (LAI) from the "MOD15A2" dataset (version 5) and NDVI and enhanced vegetation index (EVI) from the "MOD13Q1" dataset (version 5). Some preprocessing was done to obtain a high-quality NDVI dataset. First, on the basis of their quality-control information, the satellite VI data collected under unfavorable conditions (e.g., cloud and snow/ice cover) and from water bodies were filtered. Second, for each site, the 16-day composite data in pixels with a size of $2 \times 2\,\text{km}^2$ centered on the tower were composited (Xiao et al. 2008). Third, a cubic smoothing spline was used for interpolation (Horn and Schulz 2010) at points with adjacent gaps of less than 1 month, and the data were then averaged into the monthly value. After these processes, a robust method that is based on the Savitzky–Golay filter that was widely recommended for smoothing out noise in NDVI time series was used to obtain the high-quality NDVI time series. This method is to make NDVI data approach the upper NDVI envelope and to reflect the changes in NDVI patterns by an iteration process (Chen et al. 2004).

d. *Land-cover and climate types*

The classification of vegetation types at the study sites followed the 17 International Geosphere–Biosphere Programme (IGBP) land-cover types of the MODIS land-cover product (i.e., MCD12Q1), which is publicly available online (https://lpdaac.usgs.gov/). Details of this land-cover product can be found in Friedl et al. (2010). Nine different vegetation types were identified at the study sites.

TABLE 1. A description of the AmeriFlux sites used to parameterize EF in this study. More information about the sites can be found online (http://ameriflux.lbl.gov/AmeriFluxSites/Pages/Site-Map.aspx.) The MODIS NDVI product is the 16-day composite data. The multiyear average values were calculated to depict the climatological behavior of the sites. IGBP land-cover types are as in Fig. 1. Köppen–Geiger (K–G) climatic classes are as follows: the climates are arid (B), warm temperate (C), and snow (D); the precipitation is steppe (S), fully humid (f), and summer dry (s); and the temperature is cold arid (k), hot summer (a), warm summer (b), and cool summer (c).

Site	Lat (°)	Lon (°)	Elev (m)	IGBP	K–G	H ($W m^{-2}$)	LE ($W m^{-2}$)	T_a (°C)	WS ($m s^{-1}$)	RH (%)	NDVI	Reference
						Deciduous forests						
US-MOz	38.74	−92.20	219.4	DBF	Cfa	36.73	54.54	13.24	2.71	67.53	0.67	Gu et al. (2007)
US-Slt	39.91	−74.60	30	DBF	Cfa	46.19	51.77	12.48	1.91	68.26	0.70	Clark et al. (2010)
US-UMB	45.56	−84.71	234	DBF	Dfb	34.42	33.88	6.81	3.72	69.48	0.69	Curtis et al. (2002)
US-UMd	45.56	−84.70	239	DBF	Dfb	34.14	33.06	7.45	2.78	72.67	0.70	Hardiman et al. (2011)
US-WBW	35.96	−84.29	343	DBF	Cfa	35.31	48.58	14.72	2.18	68.39	0.66	Wilson and Meyers (2007)
US-WCr	45.91	−90.08	515	DBF	Dfb	31.25	30.30	5.82	2.64	86.14	0.66	Shaw et al. (2004)
US-PFa	45.95	−90.27	470	MF	Dfb	22.28	33.80	6.08	3.40	75.79	0.71	Ricciuto et al. (2008)
US-Syv	46.24	−89.35	540	MF	Dfb	22.11	26.91	4.99	3.15	72.28	0.71	Desai et al. (2005)
						Evergreen forests						
US-Ho1	45.20	−68.74	60	ENF	Dfb	36.18	30.62	6.58	2.63	66.95	0.79	Hollinger et al. (1999)
US-Ho2	45.21	−68.75	91	ENF	Dfb	42.21	35.62	6.52	2.63	67.40	0.80	Hollinger et al. (2004)
US-Ho3	45.21	−68.73	61	ENF	Dfb	54.70	43.05	6.33	2.61	67.05	0.75	Hollinger et al. (2004)
US-NC1	35.81	−76.71	5	ENF	Cfa	27.74	63.67	15.65	1.87	73.58	0.75	Domec et al. (2009)
US-NC2	35.80	−76.67	12	ENF	Cfa	26.12	79.59	16.01	1.99	70.54	0.75	Domec et al. (2009)
US-Vcm	35.89	−106.53	3003	ENF	Dfb	64.79	45.08	4.53	2.93	49.82	0.56	Molotch et al. (2009)
US-Skr	25.36	−81.08	1	EBF	Cwa	32.96	95.26	23.56	2.05	77.74	0.84	Barr et al. (2012)
						Shrublands						
CA-NS6	55.92	−98.96	244	OSH	Dfc	27.87	19.39	−0.84	2.41	70.74	0.63	Goulden et al. (2006)
CA-NS7	56.64	−99.95	297	OSH	Dfc	40.18	26.46	−0.87	1.39	69.37	0.58	Goulden et al. (2006)
US-Mpj	34.44	−106.24	2138	OSH	BSk	75.58	28.86	10.34	3.36	44.61	0.41	Xiao et al. (2008)
US-SRC	31.91	−110.84	991	OSH	BSk	57.71	23.85	20.12	2.22	49.66	0.22	Kurc and Benton (2010)
US-Whs	31.74	−110.05	1370	OSH	BSk	63.70	20.75	17.53	3.07	37.46	0.21	Scott (2010)
US-Wjs	34.43	−105.86	1926	OSH	BSk	64.39	29.95	13.00	3.57	45.60	0.24	Xiao et al. (2008)
						Grasslands						
US-AR1	36.43	−99.42	611	GRA	Cfa	36.40	53.69	15.86	3.62	70.53	0.39	Billesbach (2011)
US-AR2	36.64	−99.60	646	GRA	BSk	44.96	35.98	15.75	4.13	69.57	0.38	Billesbach (2011)
US-ArB	35.55	−98.04	424	GRA	Cfa	44.36	55.27	18.20	3.81	65.66	0.51	Schmidt et al. (2011)
US-ArC	35.55	−98.04	424	GRA	Cfa	42.47	64.36	17.78	4.13	66.16	0.50	Schmidt et al. (2011)
US-Bkg	44.35	−96.84	510	GRA	Dfa	18.65	63.70	6.23	3.51	77.01	0.51	Gilmanov et al. (2005)
US-CaV	39.06	−79.42	994	GRA	Cfb	14.13	30.37	7.40	2.59	80.60	0.61	Hollinger et al. (2010)
US-Cop	38.09	−109.39	1520	GRA	BSk	48.94	14.61	13.29	2.17	45.51	0.21	Bowling et al. (2010)
US-Dk1	35.97	−79.09	168	GRA	Cfa	25.08	53.45	14.99	1.55	70.37	0.72	Stoy et al. (2005)
US-FPe	48.31	−105.10	634	GRA	BSk	27.86	27.60	5.10	3.12	71.88	0.32	Schmidt et al. (2011)
US-Fwf	35.45	−111.77	2270	GRA	Csb	30.95	31.18	8.48	4.00	45.61	0.37	Dore et al. (2012)
US-IB2	41.84	−88.24	226	GRA	Dfa	17.19	51.01	9.33	2.75	72.36	0.53	Matamala et al. (2008)
US-KUT	45.00	−93.19	301	GRA	Dfa	3.19	41.93	6.77	2.39	66.84	0.58	Hiller et al. (2011)
US-Sdh	42.10	−101.41	1081	GRA	Dsb	25.02	63.56	9.66	3.97	65.53	0.31	Billesbach (2011)
US-Seg	34.36	−106.70	1622	GRA	BSk	54.25	21.31	13.27	3.01	41.23	0.18	Muldavin et al. (2008)
US-Var	38.41	−120.95	129	GRA	Csa	54.15	25.03	15.72	1.33	61.80	0.51	Ma et al. (2007)
US-FR2	29.95	−98.00	271.9	WSA	Cfa	56.21	47.92	20.18	2.11	65.37	0.59	Schmidt et al. (2011)
US-SRM	31.82	−110.87	1116	WSA	BSk	63.86	26.28	18.98	2.61	34.29	0.26	Cavanaugh et al. (2011)
US-Ton	38.43	−120.97	177	WSA	Csa	64.79	32.12	16.51	2.20	57.52	0.50	Ma et al. (2007)
						Cropland						
US-ARM	36.61	−97.49	314	CRO	Cfa	32.16	43.32	15.03	4.35	66.24	0.46	Lokupitiya et al. (2009)
US-Br3	41.97	−93.69	314	CRO	Dfa	16.61	49.50	9.35	3.37	75.60	0.45	Hernandez-Ramirez et al. (2011)
US-Ne2	41.16	−96.47	362	CRO	Dfa	20.90	52.13	10.18	3.45	76.72	0.50	Verma et al. (2005)
US-Ne3	41.18	−96.44	363	CRO	Dfa	24.43	48.14	10.19	3.50	72.49	0.49	Verma et al. (2005)

TABLE 2. As in Table 1, but for the AmeriFlux sites used to evaluate the accuracy of the EF parameterizations in this study.

Site	Lat (°)	Lon (°)	Elev (m)	IGBP	K–G	H (W m^{-2})	LE (W m^{-2})	T_a (°C)	WS (m s^{-1})	RH (%)	NDVI	Reference
						Deciduous forests						
US-Bar	44.06	−71.29	272	DBF	Dfb	35.74	36.81	7.48	1.34	74.73	0.71	Jenkins et al. (2007)
US-Bn2	63.92	−145.37	410	DBF	Dsc	19.49	25.29	1.32	3.06	65.74	0.57	Liu and Randerson (2008)
US-Chr	35.93	−84.33	286	DBF	Cfa	37.56	45.55	15.39	2.86	65.77	0.69	Schmidt et al. (2011)
US-Dk2	35.97	−79.10	168	DBF	Cfa	24.44	57.23	15.30	2.13	68.13	0.71	Stoy et al. (2005)
US-Ha1	42.54	−72.17	340	DBF	Dfb	32.65	37.03	8.09	2.31	73.23	0.75	Urbanski et al. (2007)
US-MMS	39.32	−86.41	275	DBF	Cfa	26.65	42.30	12.37	3.57	70.63	0.68	Dragoni et al. (2007)
US-Dix	39.97	−74.43	48	MF	Cfa	52.51	34.70	12.45	1.93	67.56	0.66	Clark et al. (2010)
US-GMF	41.97	−73.23	493	MF	Dfb	34.38	30.09	7.11	2.76	73.55	0.74	Schmidt et al. (2011)
						Evergreen forests						
CA-NS1	55.88	−98.48	253	ENF	Dfc	36.56	19.56	1.77	2.57	71.68	0.66	Goulden et al. (2006)
CA-NS2	55.91	−98.52	257	ENF	Dfc	45.32	23.48	−0.93	2.96	70.45	0.68	Goulden et al. (2006)
CA-NS5	55.86	−98.49	254	ENF	Dfc	27.04	23.54	−1.45	1.85	72.49	0.67	Goulden et al. (2006)
US-Blk	44.16	−103.65	1718	ENF	Dfb	44.81	40.14	6.54	2.41	57.17	0.66	Schmidt et al. (2011)
US-Bn1	63.89	−145.74	518	ENF	Dsc	35.80	28.95	1.63	2.59	65.96	0.57	Liu and Randerson (2008)
US-Fmf	35.14	−111.73	2160	ENF	Csb	56.87	36.96	9.76	2.22	44.15	0.53	Dore et al. (2008)
US-Fuf	35.09	−111.76	2180	ENF	Csb	68.68	39.35	9.01	2.55	45.38	0.57	Román et al. (2009)
US-SP2	29.76	−82.24	43	ENF	Cfa	42.83	71.11	19.37	1.29	76.05	0.73	Gholz and Clark (2002)
BR-Sa1	−2.86	−54.96	88	EBF	Am	20.22	87.85	25.97	2.16	84.44	0.87	Hutyra et al. (2008)
BR-Sa3	−3.02	−54.97	100	EBF	Am	23.40	100.04	25.87	2.21	74.63	0.86	Hutyra et al. (2008)
						Shrublands						
US-Bn3	63.92	−145.75	469	OSH	Dsc	20.65	23.58	2.12	2.80	64.13	0.52	Liu and Randerson (2008)
US-ICt	68.61	−149.30	930	OSH	ET	24.14	32.91	2.52	2.53	71.23	0.57	Euskirchen et al. (2007)
US-Ses	34.33	−106.74	1593	OSH	BSk	55.77	20.43	14.34	2.68	39.58	0.18	Muldavin et al. (2008)
US-Ced	39.84	−74.38	58	CSH	Cfa	41.99	53.89	12.48	2.17	69.25	0.69	Clark et al. (2009)
US-KS2	28.61	−80.67	6	CSH	Cfa	37.81	69.82	22.21	1.94	77.71	0.64	Powell et al. (2008)
US-Los	46.08	−89.98	480	CSH	Dfb	25.81	25.42	3.02	2.68	70.83	0.67	Sulman et al. (2009)
US-SO2	33.37	−116.62	1394	CSH	Csa	94.83	32.04	14.32	2.19	44.77	0.41	Luo et al. (2007)
US-SO4	33.38	−116.64	1394	CSH	Csa	95.51	28.72	14.80	2.06	44.75	0.41	Luo et al. (2007)
						Grasslands						
US-Aud	31.59	−110.51	1469	GRA	BSk	53.19	22.25	16.25	2.58	46.32	0.25	Wilson and Meyers (2007)
US-Ctn	43.95	−101.85	744	GRA	BSk	39.25	45.50	9.33	4.09	62.82	0.34	Schmidt et al. (2011)
US-Dia	37.68	−121.53	323	GRA	csa	41.89	18.18	16.01	2.99	51.72	0.36	van Gorsel et al. (2009)
US-Goo	34.25	−89.77	87	GRA	Cfa	26.73	57.01	16.66	1.67	80.28	0.67	Wilson and Meyers (2007)
US-KFS	39.06	−95.19	333	GRA	Cfa	22.39	47.21	13.61	2.80	70.46	0.56	Brunsell et al. (2008)
US-Kon	39.08	−96.56	443	GRA	Cfa	21.55	46.29	14.32	3.95	67.21	0.49	Brunsell et al. (2008)
US-Wkg	31.74	−109.94	1531	GRA	BSk	58.92	20.91	17.37	3.80	35.17	0.22	Krishnan et al. (2012)
US-Wlr	37.52	−96.86	408	GRA	Cfa	28.04	51.98	13.60	3.46	68.40	0.47	Jastrow et al. (2000)
						Cropland						
US-Bo1	40.01	−88.29	219	CRO	Dfa	26.76	50.40	11.14	4.37	79.59	0.45	Hollinger et al. (2005)
US-Bo2	40.01	−88.29	219.3	CRO	Dfa	27.24	40.58	12.85	3.16	70.82	0.46	Meyers and Hollinger (2004)
US-Br1	41.69	−93.69	275	CRO	Dfa	18.84	51.66	9.07	3.44	75.84	0.60	Hernandez-Ramirez et al. (2011)
US-IB1	41.86	−88.22	225	CRO	Dfa	21.11	51.60	9.85	3.10	72.39	0.50	Matamala et al. (2008)

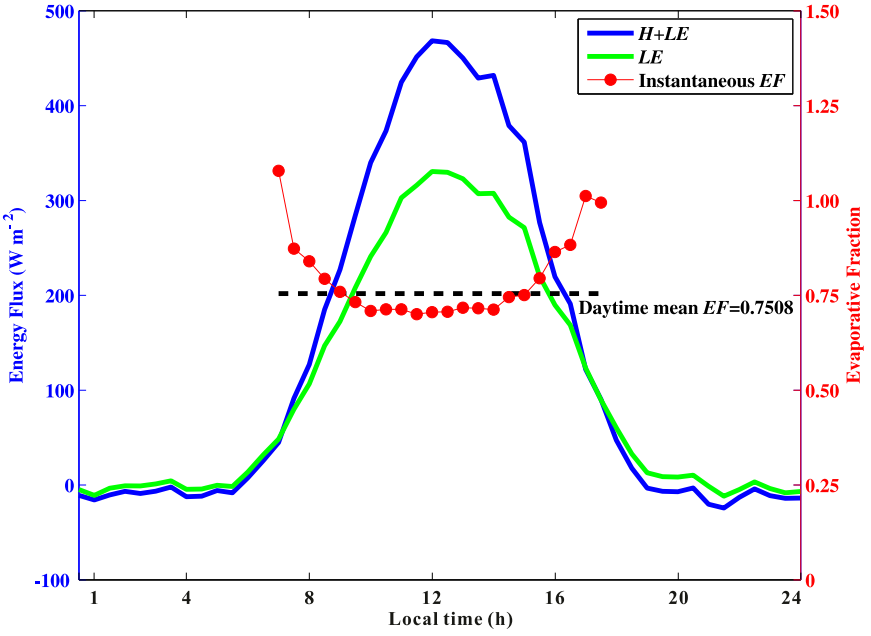

FIG. 2. The diurnal cycle of available energy (H plus LE), LE, and EF during the daytime at the US-NC1 site (35.81°N, 76.71°W; land-cover type: evergreen needleleaf forest). The red dots are calculated by the fluxes at moment t, demonstrating little variance in daytime EF. The black dashed line is a daytime mean (0.75) calculated from the summation of monthly diurnal fluxes [i.e., Eq. (2)].

The world map of the Köppen–Geiger classification of climate, which displays 31 types of climate at a resolution of 0.5° × 0.5° on the basis of temperature and precipitation observations for the period of 1951–2000 (Kottek et al. 2006), was used to extract the climatic information for each site (Tables 1 and 2). The usable digital map is provided freely online (http://koeppen-geiger.vu-wien.ac.at/).

e. *Calculation of monthly EF*

Although the EC method suffers an important issue of energy imbalance, that is, the sum of LE and H is not equal to $R_n - G$, most applications and correction methods assume that the Bowen ratio is kept for the EC method (Twine et al. 2000; Wang and Dickinson 2012; Wilson et al. 2002). Under this assumption, EF is independent of the energy-closure problem and does not need correction. Monthly EF here is obtained to estimate the long-term variance of EF, which not only avoids the effect of the average error from daily to monthly EF but also makes the following parameterizations (in section 3b) globally applicable because most climatic datasets—for example, those used as input data for the parameterization—are only available at monthly scale.

Unlike the sinusoidal variation in available energy (LE plus H), the EF remains almost constant during the daytime under fair-weather conditions (Fig. 2) (Brutsaert and Sugita 1992; Crago 1996; Gentine et al. 2007; Nichols and Cuenca 1993) and isolates soil and plant moisture resistances to energy partitioning. Existing studies indicate that EF has a diurnal U-shaped pattern that is partly due to the diurnal variation in RH or WS (Gentine et al. 2011, 2007; Lhomme and Elguero 1999). Further studies show that in the early morning and late afternoon the fraction of diffuse solar radiation to total solar radiation is higher and diffuse solar radiation is more efficiently absorbed by vegetation for photosynthesis, resulting in a higher EF (Wang et al. 2008). This is similar to the results of Smith et al. (1992) that show that cloudiness induces significant variance in the energy budget to control the EF. In addition, the values of LE and H in the night are small enough to be ignored. Therefore, this study focuses on the biological and environmental controls on monthly daytime EF. Monthly daytime EF is calculated with (Peng et al. 2013)

$$\mathrm{EF} = \frac{\int_{\text{sunrise}}^{\text{sunset}} \mathrm{LE}_{t,\text{monthlymean}}(t)\,dt}{\int_{\text{sunrise}}^{\text{sunset}} [H_{t,\text{monthlymean}}(t) + \mathrm{LE}_{t,\text{monthlymean}}(t)]\,dt}, \quad (2)$$

where sunset and sunrise, expressed as local time, can be calculated as a function of site latitude, month, and

day (available online at http://herbert.gandraxa.com/length_of_day.xml), ensuring a restrained variation in EF and a positive available energy; $LE_{t,monthlymean}$ and $H_{t,monthlymean}$ are the monthly means of instantaneous LE and H, respectively, at time t. The EF ranges from 0 to 1. An EF value of 0.0 indicates a very dry surface (e.g., dry desert) with no evapotranspiration from soils and plants, and an EF value of 1.0 indicates a very wet (e.g., water body) or highly vegetated surface. In addition, the monthly means of all other variables were calculated by averaging the monthly diurnal cycles.

f. Partial correlation analysis

To identify further the impacts of individual parameters on monthly EF, a partial correlation analysis was applied to statistically remove the effect of other factors (Cohen et al. 2013); partial correlation coefficients ρ at a significance level p of 0.05 were used. To parameterize the monthly EF, a stepwise-regression model was applied at a p of 0.05 for entry and 0.1 for removal to avoid collinearity with in-model variables at a p of 0.1 (Montgomery et al. 2012). A stepwise regression is a systematic method for adding and removing terms from a multilinear model on the basis of their statistical significance in a regression. At each step, the p value of an F statistic is computed to test models with and without a potential variable. The model proceeds as follows:

1) Fit the initial model with the most explanatory power variable.
2) If any variables not in the model have p values of less than 0.05 (forward selection), add the one with the smallest p value and repeat this step; otherwise, go to step 3.
3) If any variables in the model have p values greater than 0.1 (backward elimination), remove the one with the largest p value and go to step 2; otherwise, end.

After these three steps, no more variables can be entered and removed. To quantify the collinearity of in-model variables, the variance inflation factor (VIF) is recommended as a criterion, and its value in excess of 10 is a threshold for an unreliable regression (Chatterjee and Price 1977). Also, the correlation coefficient r at a p of 0.05 and root-mean-square error (RMSE) were used to evaluate the accuracy of fitting and parameterization of monthly EF.

g. Selection of determining variables

The LE is strongly controlled by vegetation-growth demand, atmospheric demand, and water supply (Bucci et al. 2008; Chang et al. 2006; Hu et al. 2009; Maximov et al. 2008; Monteith 1965; Saugier et al. 1997; Si et al. 2007; Tanaka et al. 2008; Wang et al. 2010, 2007; Wang and Liang 2008; Zha et al. 2010), including r_c, VI, RH, R_n, T_a, vapor pressure deficit, WS, and soil moisture (SM). On the basis of the physical simplification of EF, standardized by its definition of $EF = LE/(R_n - G)$ (Wang and Liang 2009; Wang et al. 2010), the relationships between EF and vegetation demand (expressed by VI), atmospheric demand (expressed by T_a, DTR, and WS), and water supply (expressed by SM or RH) were investigated. These factors are as independent as possible and have specific physical meanings.

Three similar temperature measurements are available: the maximum air temperature T_{max}, minimum air temperature T_{min}, and daily mean air temperature. The correlation between EF and T_{min} is slightly better than those of EF with T_{max} and averaged air temperature at monthly scale, likely because T_{min} may control respiratory enzyme activity. The T_{min} data have been widely collected at weather stations and are easily accessible; therefore, T_{min} was analyzed in this study. Similarly, the partial correlation between EF and NDVI is a little better than those of EF with EVI and LAI. The availability of NDVI is much higher than that of EVI and LAI; therefore, the results using the NDVI are reported in this study.

In developing the equations to calculate EF and based on the findings mentioned in section 3a, the 81 sites were divided into five categories: deciduous forests, evergreen forests, shrublands, grasslands, and cropland. An empirical equation was created for each category with climatic parameters (T_{min}, DTR, WS, RH) and satellite vegetation index (NDVI) as input data. It is found that the equations derived from such a process can well reflect the impacts of land-cover types and climates on EF (section 3b).

3. Results

a. Biological and environmental controls on monthly EF

The analyses in this section aim to identify the relationships between EF and biological/environmental parameters but cannot determine the causes or results. These relationships can actually be a mixture of cause and result. Such analyses at daily and monthly scales were conducted, and similar conclusions were derived. To coordinate with the following parameterizations of monthly EF for its long-term variance, the results at monthly scale are reported here.

Figure 3 shows the typical scatterplots of monthly EF against monthly T_{min}, NDVI, RH, DTR, and WS for deciduous forests, evergreen forests, shrublands,

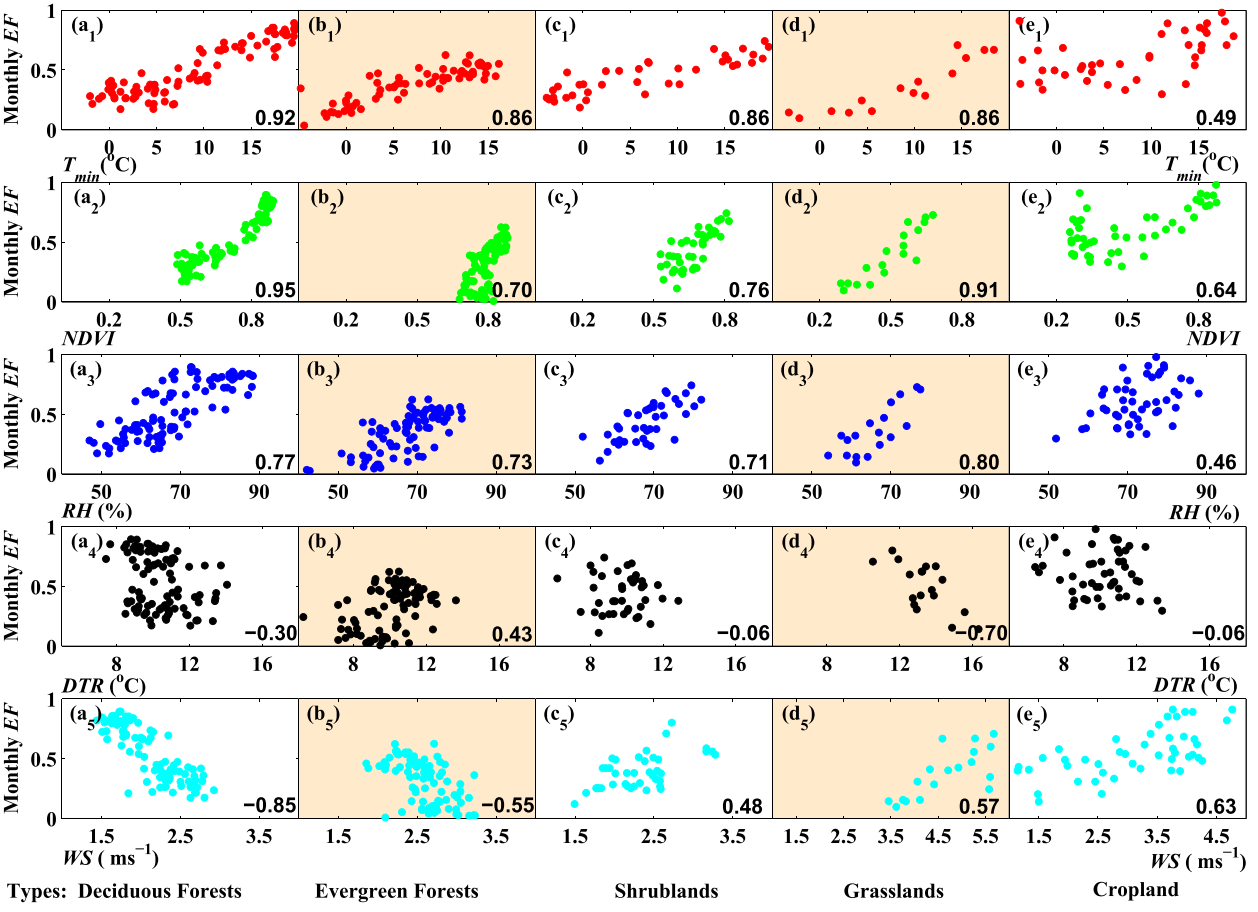

FIG. 3. Scatterplots of monthly EF against T_{min}, NDVI, RH, DTR, and WS for the example sites US-Dk2 (35.97°N, 79.10°W), US-Ho1 (45.20°N, 68.74°W), US-Ced (39.84°N, 74.38°W), US-ArB (35.55°N, 98.04°W), and US-IB1 (41.86°N, 88.22°W), representing the five land-cover types of deciduous forests, evergreen forests, shrublands, grasslands, and cropland, respectively. The red, green, blue, black, and cyan dots represent the relationships of monthly EF with T_{min}, NDVI, RH, DTR, and WS, respectively. The corresponding correlation coefficient is shown at the bottom right of each panel.

grasslands, and cropland sites. In general, vegetation influences water and heat exchange through biophysical and ecophysiological responses to different environmental conditions. In different ecosystems and climates, the magnitude and mode of these responses are obviously inconsistent (Wang and Dickinson 2012). With the exception of cropland (Fig. 3e1), monthly EF increases linearly with T_{min}; the different result for cropland is partly due to agricultural management (e.g., irrigation during seeding periods). The NDVI loses its sensitivity to vegetation coverage when vegetation is dense (Wang et al. 2010); thus, monthly EF increases at a greater rate at high NDVI than at low NDVI in deciduous forests (Fig. 3a2). Because of crop growth and transpiration demand, monthly EF increases linearly with NDVI in cropland sites with high NDVI, whereas significant soil evaporation may contribute to the high monthly EF when the NDVI is low (Fig. 3e2) in the seeding period.

Monthly EF agrees well with RH (Figs. 3a3,b3,c3,d3,e3), which represents impacts of surface aridity (or soil moisture) and water vapor deficit on LE. The DTR is negatively related to monthly EF because as the amount of energy heating Earth's surface increases it makes T_{max} high and then DTR large, and thus energy consumption by LE decreases; consequently, monthly EF decreases (Figs. 3a4,b4,c4,d4,e4). DTR also is closely related to surface aridity or soil moisture (Mu et al. 2007b; Wang and Liang 2008).

The monthly EF values over forests and grasslands have different responses to WS. To be specific, monthly EF negatively correlates with WS over deciduous and evergreen forests but positively correlates over shrublands, grasslands, and cropland (Figs. 3a5,b5,c5,d5,e5). This opposite correlation over different land-cover types results from the complicated effects of WS on LE (e.g., transpiration) and H through the intricate impacts of WS on the aerodynamic resistance, leaf

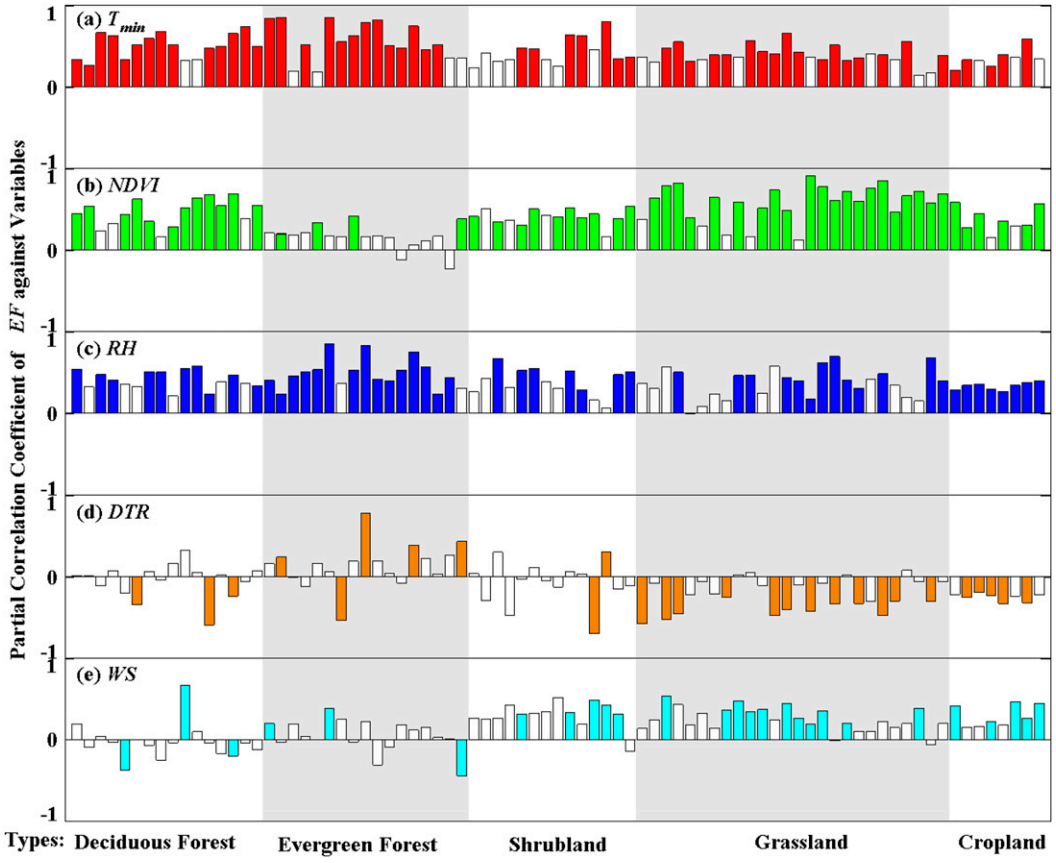

FIG. 4. The partial correlation coefficients of monthly EF with (a) $T_{\min}$, (b) NDVI, (c) RH, (d) DTR, and (e) WS for the five vegetation classes (deciduous forests, evergreen forests, shrublands, grasslands, and cropland). The white bar represents a partial correlation that does not pass the t test at a significance level of 0.05, and the bars with other colors pass that test. Each bar in the figure represents one station in Tables 1 and 2.

boundary layer resistance, and stomatal resistance (Dixon and Grace 1984; Gutiérrez et al. 1994). The stomatal resistance increases by ~40% with an increase of ~0.7–4.7 m s^{-1} in WS in a mixed broadleaved deciduous forest (Kim et al. 2014), whereas the aerodynamic resistance decreases in forests and grasslands; thus, the EF decreases more dramatically with WS in the forest region. Lei et al. (2010) reported that WS accelerates the transpiration of *Artemisia ordosica* (a shrub) in the Tengger Desert of China. Therefore, the relationship between EF and WS depends on the aerodynamic resistance and r_c to thermal and vapor transfer. In all, the aerodynamic resistance decreases with increasing WS as based on the MOST, and the r_c increases with increasing WS as based on the rearranged Penman–Monteith equation.

Figure 4 displays the partial correlation coefficients ρ of monthly EF with $T_{\min}$, NDVI, RH, DTR, and WS at all of the sites. In comparing the results over each land-cover type shown in Fig. 4 with each other and trying our best to merge different land-cover types into a class, the study sites were divided into five categories: deciduous forests, evergreen forests, shrublands, grasslands, and cropland. Strong relationships are observed between monthly EF and $T_{\min}$, NDVI, and RH in deciduous forests, with site-averaged ρ values of 0.53, 0.52, and 0.46 ($p < 0.05$), respectively (Fig. 4). When compared with deciduous forests, stronger relationships are found between monthly EF and $T_{\min}$ and NDVI in evergreen forests, with site-averaged ρ values of 0.65 and 0.51 ($p < 0.05$), respectively. Monthly EF is less sensitive to NDVI in evergreen forests because of the low perennial variance of NDVI. Similarly, $T_{\min}$, RH, NDVI, and WS mainly control monthly EF in shrublands, with site-averaged ρ values of 0.53, 0.50, 0.42, and −0.37 ($p < 0.05$), respectively. The strongest correlation of monthly EF with NDVI occurs in grasslands, with a site-averaged ρ of 0.66 ($p < 0.05$); similar relationships among RH, $T_{\min}$, DTR, and WS and monthly EF are observed for grasslands, with site-averaged ρ values of 0.46, 0.44, −0.40, and 0.36 ($p < 0.05$), respectively. Because of the efficient use of water and energy by agricultural

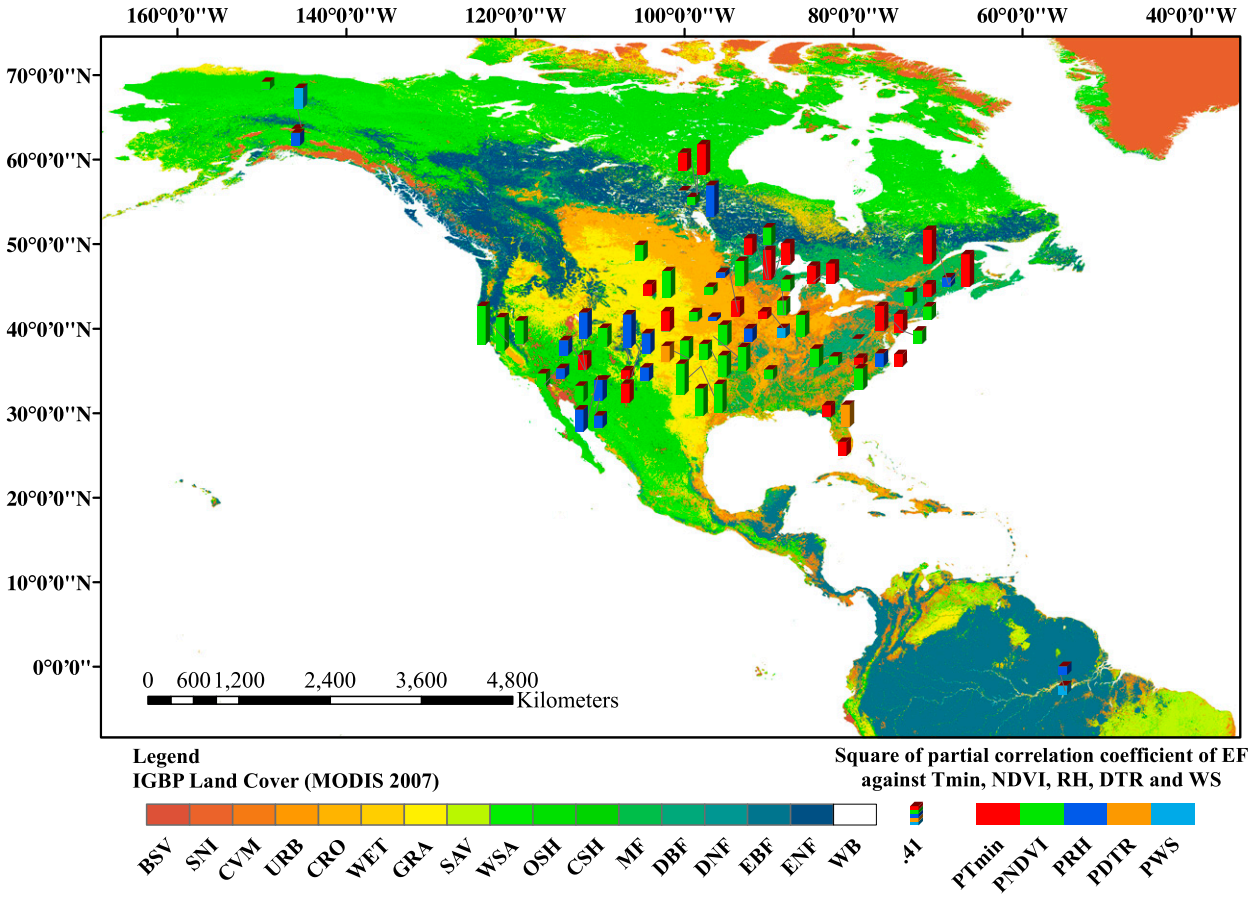

FIG. 5. The most explanatory power variable at each site is shown as a bar graph with the square of spatial correlation coefficient of monthly EF with this variable at a significance level of 0.05, on a base map of the IGBP land-cover types (MCD12Q1; 2007). IGBP types: barren or sparsely vegetated (BSV), snow ice (SNI), cropland/natural vegetation mosaics (CVM), cropland (CRO), wetland (WET), grassland (GRA), savanna (SAV), woody savanna (WSA), open shrubland (OSH), closed shrubland (CSH), mixed forest (MF), deciduous broadleaf forest (DBF), deciduous needleleaf forest (DNF), evergreen broadleaf forest (EBF), evergreen needleleaf forest (ENF), and water body (WB). Data collected at all sites in Tables 1 and 2 are shown.

management, NDVI, WS, T_{min}, RH, and DTR have very similar relationships with monthly EF in cropland, with site-averaged ρ values of 0.42, 0.36, 0.35, 0.33, and −0.27 ($p < 0.05$), respectively.

Figure 5 demonstrates the maximum explanation of monthly EF by the most explanatory power variable independently. The explanatory variance of monthly EF is defined by the square of partial correlation coefficient of monthly EF with T_{min}, NDVI, RH, DTR, and WS, ranging from 0 to 1. NDVI, T_{min}, and RH are main factors over different land-cover types, as indicated by the green, red, and blue bars, respectively (Fig. 5). The maximum variances of monthly EF explained by NDVI, T_{min}, and RH are 0.83, 0.72, and 0.71, respectively, and their means

TABLE 3. The fitted coefficients in Eq. (3) for five categories on a monthly scale are calculated by stepwise-regression models with the sites in Table 1. The correlation coefficients r and RMSE values between the measured and fitted EFs are listed. The multicollinearities among the predictor variables are evaluated by the VIF. A VIF in excess of 10 is suggested to be a criterion for an unreliable regression. An em dash indicates that this parameter does not enter the model.

Site type	a_0	a_1	a_2	a_3	a_4	a_5	r	RMSE	VIF
Deciduous forests	−0.3459	0.0147	0.5385	0.0041	—	—	0.919	0.089	3.55
Evergreen forests	0.0121	0.0169	—	0.0045	—	—	0.886	0.1003	1.28
Shrublands	−0.2791	0.0086	0.1818	0.0071	—	0.0254	0.877	0.0715	3.76
Grasslands	−0.0669	0.0036	0.6062	0.0044	−0.0171	0.0511	0.809	0.1358	2.60
Cropland	−0.1142	0.0038	0.6848	0.0078	−0.0308	0.0266	0.801	0.1142	3.36

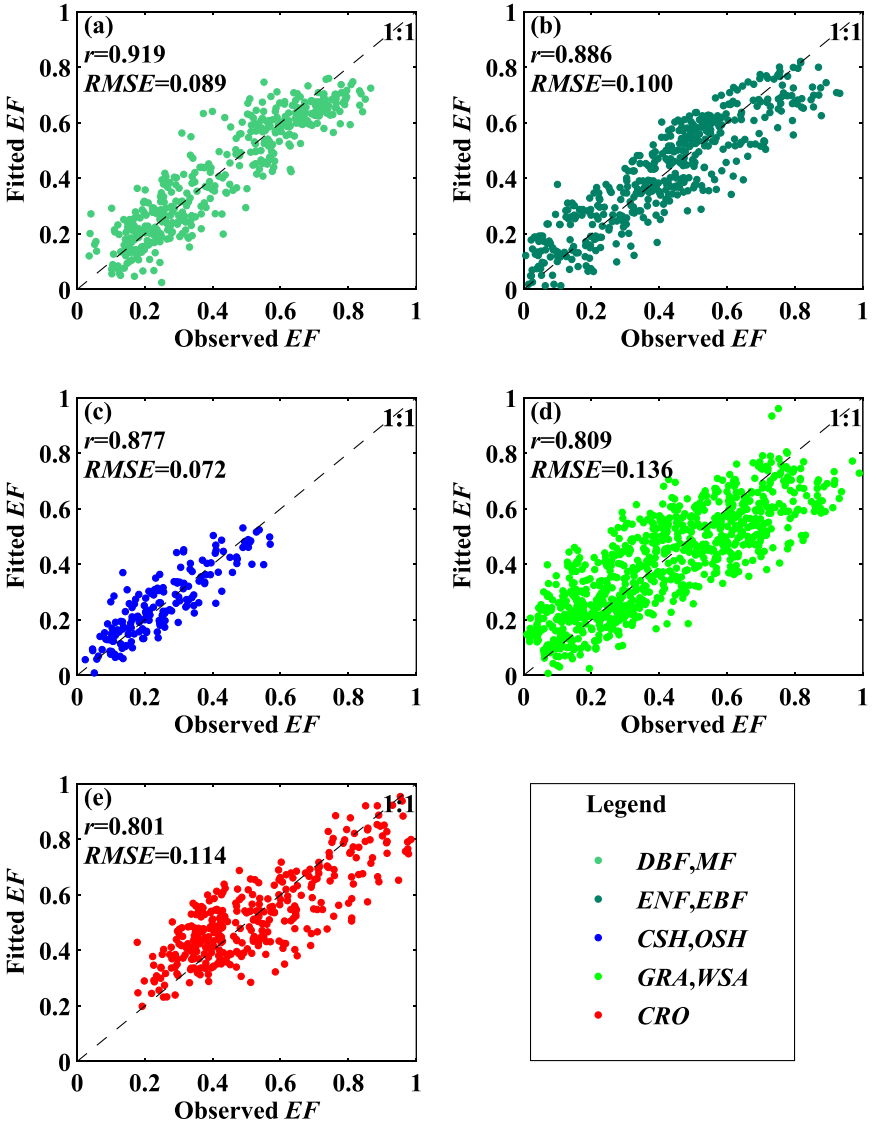

FIG. 6. The scatterplots of fitting results for (a) deciduous forests including deciduous broadleaf forests and mixed forest, (b) evergreen forests including evergreen broadleaf forest and evergreen needleleaf forest, (c) shrublands including closed shrubland and open shrubland, (d) grasslands including grassland and woody savanna, and (e) cropland. Using the data collected at sites in Table 1, the monthly EF is fitted by the stepwise-regression model [Eq. (3)]. The correlation coefficient r and RMSE are listed in each panel.

are 0.31, 0.29, and 0.23, respectively. To be more specific, 0.45 of the variance of EF can be explained by NDVI in grasslands, whereas this value is only 0.22 in forests. In contrast, $T_{\min}$ can explain 0.35 of the variance in EF in forests but only 0.20 of the variance of EF in grasslands.

b. *Empirical methods to estimate monthly EF and their validation*

The partial correlation analysis of EF against the above factors reveals that $T_{\min}$, NDVI, RH, DTR, and WS are the main factors that control monthly EF in different ecosystems. On a monthly scale, EF is fitted by stepwise-regression models with Eq. (3):

$$\mathrm{EF} = a_0 + a_1 T_{\min} + a_2 \mathrm{NDVI} + a_3 \mathrm{RH} + a_4 \mathrm{DTR} + a_5 \mathrm{WS}, \tag{3}$$

where a_i ($i = 0, 1, \ldots, 5$) is the fitted coefficient and EF is the fitting/predicted evaporative fraction.

The fitting coefficients are listed in Table 3 and are in agreement with the above correlation analysis

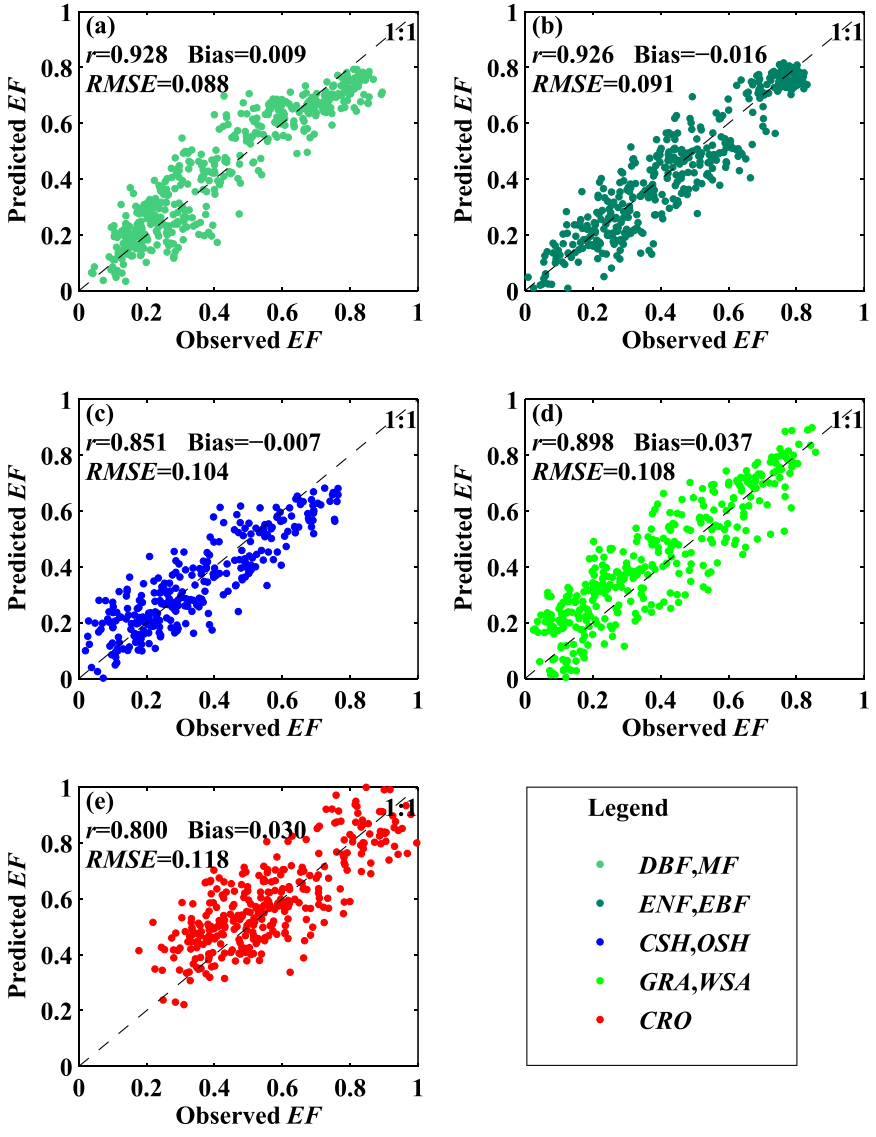

FIG. 7. Similar to Fig. 6, but for the validation results (comparison of measured and predicted monthly EF). Using the data collected at sites in Table 2, the predicted monthly EF is calculated with Eq. (3).

(section 3b). The scatterplots of the fitting results are shown in Fig. 6. For Eq. (3), the r values range from 0.80 to 0.92, and the RMSE values range from 0.07 to 0.14 for five categories. The vegetation growth has a larger impact on the EF over the deciduous forests, grasslands, and cropland than over evergreen forests and shrublands by comparison of the equation coefficients of NDVI. Moreover, WS acts to obviously promote LE for short vegetation, such as shrublands, grasslands, and cropland. The VIF that is recommended to evaluate the multicollinearity among the predictors with a threshold of 10 (Chatterjee and Price 1977) indicates that the fitting equations are reliable regression over five vegetation classes (Table 3).

Figures 7 and 8 illustrate the validation results for each site over deciduous forests, evergreen forests, shrublands, grasslands, and cropland (listed in Table 2). The predicted monthly EF values are in good agreement with the measured monthly EF values over five categories (Fig. 7). The r values between predicted and measured monthly EF range from 0.80 to 0.93, and the RMSE values range from 0.09 to 0.12 for five categories (Fig. 8). These results show that the equations for EF can be used to accurately estimate the long-term variance in EF from conventional weather

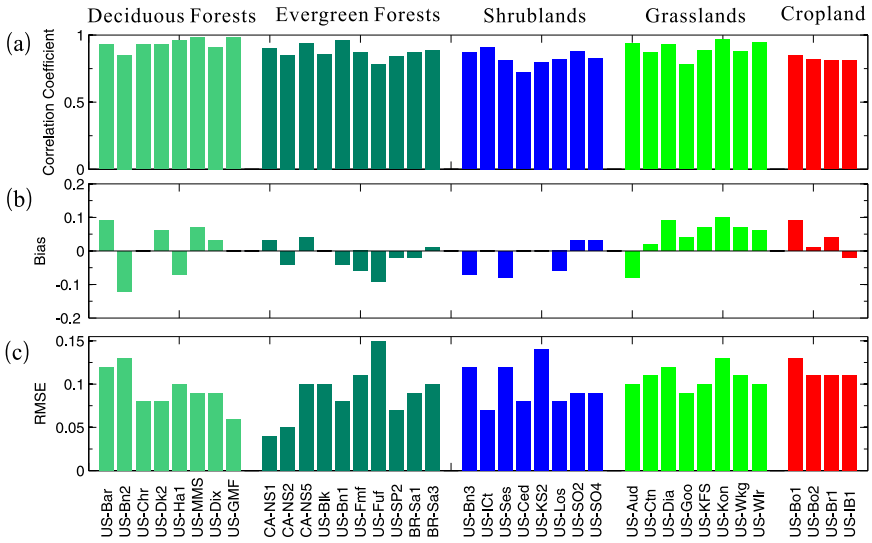

FIG. 8. The validation statistics for the measured and predicted monthly EFs calculated by Eq. (3) from the sites belonging to five vegetation classes in Table 2.

observations and NDVI, which are measured and available globally.

4. Conclusions and discussion

The objectives of this study are to identify the various factors that control monthly EF for different land-cover types and climates and to further parameterize monthly EF. Through partial correlation analyses of EF with relevant factors at 81 sites, the factors controlling monthly EF at different vegetation classes are determined as follows:

1) Positive correlations of monthly EF with T_{min}, NDVI, and RH are found for all sites, whereas the effect of WS and DTR on monthly EF is complicated and depends on land-cover type.
2) For deciduous forest sites, T_{min}, NDVI, and RH are the three main controlling factors on monthly EF and have a saturation effect at high NDVI. For evergreen forests, T_{min} and RH are the main controls. For shrubland sites, T_{min}, RH, NDVI, and WS mainly control monthly EF. For grasslands, NDVI has the best correlation with monthly EF, whereas RH, T_{min}, DTR, and WS all have similar relationships with monthly EF. Because of agricultural management, NDVI, WS, T_{min}, RH, and DTR contribute almost equally to the control of monthly EF.

In summary, the interactions between biological and environmental factors have a combined effect on monthly EF. Monthly EF can be estimated by stepwise-multiple-regression models f(NDVI, T_{min}, DTR, RH, WS), with r ranging from 0.80 to 0.92 and RMSE ranging from 0.07 to 0.14 for five categories. Model validation by comparison of predicted and observed monthly EF values indicates that the stepwise-multiple-regression models have good results.

Because T_a, WS, and RH are measured with high frequency at globally distributed stations and because NDVI can be acquired with remotely sensed data, these equations can be used to monitor global ecosystem dynamics and detect long-term trends in EF. Another advantage of these linear equations is that they are insensitive to errors of input data, unlike the nonlinear relationship of aerodynamic resistance with the environmental parameters in one- and two-source models. This study provides a preliminary study on methods to calculate EF, which is of great importance for climatic studies. High precision of parameterization is still a challenge in accurately estimating EF, and further study is needed. In addition, to obtain the global EF over all land-cover types, some effort is being made to collect the relevant data for further validation or even for developing a model of EF over the other land-cover types that were not involved in this study.

Acknowledgments. This study was funded by the National Basic Research Program of China (2012CB955302) and the National Natural Science Foundation of China (91337111, 41525018, and 41205036). AmeriFlux data were downloaded from http://ameriflux.ornl.gov/. MODIS satellite vegetation indices and land-cover-type data were downloaded from https://lpdaac.usgs.gov/. The world map of the Köppen–Geiger climatic

classification was downloaded from http://koeppen-geiger.vu-wien.ac.at/.

REFERENCES

Allen, R. G., L. S. Pereira, D. Raes, and M. Smith, 1998: Crop evapotranspiration: Guidelines for computing crop water requirements. U.N. Food and Agriculture Organization Irrigation and Drainage Paper 56, 300 pp. [Available online at http://www.fao.org/docrep/x0490e/x0490e00.htm.]

Amidan, B. G., T. A. Ferryman, and S. K. Cooley, 2005: Data outlier detection using the Chebyshev theorem. *Proc. 2005 IEEE Aerospace Conf.*, Big Sky, MT, IEEE, 3814–3819, doi:10.1109/AERO.2005.1559688.

Bailey, B., J. Montero, C. Biel, D. Wilkinson, A. Anton, and O. Jolliet, 1993: Transpiration of *Ficus benjamina*: Comparison of measurements with predictions of the Penman–Monteith model and a simplified version. *Agric. For. Meteor.*, **65**, 229–243, doi:10.1016/0168-1923(93)90006-4.

Baldocchi, D., and Coauthors, 2001: FLUXNET: A new tool to study the temporal and spatial variability of ecosystem–scale carbon dioxide, water vapor, and energy flux densities. *Bull. Amer. Meteor. Soc.*, **82**, 2415–2434, doi:10.1175/1520-0477(2001)082<2415:FANTTS>2.3.CO;2.

Barr, J. G., V. Engel, T. J. Smith, and J. D. Fuentes, 2012: Hurricane disturbance and recovery of energy balance, CO_2 fluxes and canopy structure in a mangrove forest of the Florida Everglades. *Agric. For. Meteor.*, **153**, 54–66, doi:10.1016/j.agrformet.2011.07.022.

Best, M. J., and Coauthors, 2015: The plumbing of land surface models: Benchmarking model performance. *J. Hydrometeor.*, **16**, 1425–1442, doi:10.1175/JHM-D-14-0158.1.

Billesbach, D. P., 2011: Estimating uncertainties in individual eddy covariance flux measurements: A comparison of methods and a proposed new method. *Agric. For. Meteor.*, **151**, 394–405, doi:10.1016/j.agrformet.2010.12.001.

Bowling, D. R., S. Bethers-Marchetti, C. K. Lunch, E. E. Grote, and J. Belnap, 2010: Carbon, water, and energy fluxes in a semiarid cold desert grassland during and following multiyear drought. *J. Geophys. Res.*, **115**, G04026, doi:10.1029/2010JG001322.

Brunsell, N. A., J. M. Ham, and C. E. Owensby, 2008: Assessing the multi-resolution information content of remotely sensed variables and elevation for evapotranspiration in a tall-grass prairie environment. *Remote Sens. Environ.*, **112**, 2977–2987, doi:10.1016/j.rse.2008.02.002.

Brutsaert, W., and M. Sugita, 1992: Application of self-preservation in the diurnal evolution of the surface energy budget to determine daily evaporation. *J. Geophys. Res.*, **97**, 18 377–18 382, doi:10.1029/92JD00255.

Bucci, S. J., F. G. Scholz, G. Goldstein, W. A. Hoffmann, F. C. Meinzer, A. C. Franco, T. Giambelluca, and F. Miralles-Wilhelm, 2008: Controls on stand transpiration and soil water utilization along a tree density gradient in a neotropical savanna. *Agric. For. Meteor.*, **148**, 839–849, doi:10.1016/j.agrformet.2007.11.013.

Cavanaugh, M. L., S. A. Kurc, and R. L. Scott, 2011: Evapotranspiration partitioning in semiarid shrubland ecosystems: A two-site evaluation of soil moisture control on transpiration. *Ecohydrology*, **4**, 671–681, doi:10.1002/eco.157.

Cerveny, R. S., J. Lawrimore, R. Edwards, and C. Landsea, 2007: Extreme weather records: Compilation, adjudication, and publication. *Bull. Amer. Meteor. Soc.*, **88**, 853–860, doi:10.1175/BAMS-88-6-853.

Chang, X., W. Zhao, Z. Zhang, and Y. Su, 2006: Sap flow and tree conductance of shelter-belt in arid region of China. *Agric. For. Meteor.*, **138**, 132–141, doi:10.1016/j.agrformet.2006.04.003.

Chatterjee, S., and B. Price, 1977: *Regression Analysis by Example.* John Wiley and Sons, 228 pp.

Chen, J., P. Jönsson, M. Tamura, Z. Gu, B. Matsushita, and L. Eklundh, 2004: A simple method for reconstructing a high-quality NDVI time-series data set based on the Savitzky–Golay filter. *Remote Sens. Environ.*, **91**, 332–344, doi:10.1016/j.rse.2004.03.014.

Clark, K. L., and Coauthors, 2009: Decision support tools to improve the effectiveness of hazardous fuel reduction treatments in the New Jersey Pine Barrens. *Int. J. Wildland Fire*, **18**, 268–277, doi:10.1071/WF08080.

——, N. Skowronski, and J. Hom, 2010: Invasive insects impact forest carbon dynamics. *Global Change Biol.*, **16**, 88–101, doi:10.1111/j.1365-2486.2009.01983.x.

Cohen, J., P. Cohen, S. G. West, and L. S. Aiken, 2013: *Applied Multiple Regression/Correlation Analysis for the Behavioral Sciences.* Routledge, 703 pp.

Crago, R. D., 1996: Conservation and variability of the evaporative fraction during the daytime. *J. Hydrol.*, **180**, 173–194, doi:10.1016/0022-1694(95)02903-6.

Curtis, P. S., P. J. Hanson, P. Bolstad, C. Barford, J. Randolph, H. Schmid, and K. B. Wilson, 2002: Biometric and eddy-covariance based estimates of annual carbon storage in five eastern North American deciduous forests. *Agric. For. Meteor.*, **113**, 3–19, doi:10.1016/S0168-1923(02)00099-0.

Desai, A. R., P. V. Bolstad, B. D. Cook, K. J. Davis, and E. V. Carey, 2005: Comparing net ecosystem exchange of carbon dioxide between an old-growth and mature forest in the upper Midwest, USA. *Agric. For. Meteor.*, **128**, 33–55, doi:10.1016/j.agrformet.2004.09.005.

Dixon, M., and J. Grace, 1984: Effect of wind on the transpiration of young trees. *Ann. Bot.*, **53**, 811–819.

Domec, J.-C., A. Noormets, J. S. King, G. Sun, S. G. McNulty, M. J. Gavazzi, J. L. Boggs, and E. A. Treasure, 2009: Decoupling the influence of leaf and root hydraulic conductances on stomatal conductance and its sensitivity to vapour pressure deficit as soil dries in a drained loblolly pine plantation. *Plant Cell Environ.*, **32**, 980–991, doi:10.1111/j.1365-3040.2009.01981.x.

Dore, S., and Coauthors, 2008: Long-term impact of a stand-replacing fire on ecosystem CO_2 exchange of a ponderosa pine forest. *Global Change Biol.*, **14**, 1801–1820, doi:10.1111/j.1365-2486.2008.01613.x.

——, M. Montes-Helu, S. C. Hart, B. A. Hungate, G. W. Koch, J. B. Moon, A. J. Finkral, and T. E. Kolb, 2012: Recovery of ponderosa pine ecosystem carbon and water fluxes from thinning and stand-replacing fire. *Global Change Biol.*, **18**, 3171–3185, doi:10.1111/j.1365-2486.2012.02775.x.

Dragoni, D., H. P. Schmid, C. S. B. Grimmond, and H. W. Loescher, 2007: Uncertainty of annual net ecosystem productivity estimated using eddy covariance flux measurements. *J. Geophys. Res.*, **112**, D17102, doi:10.1029/2006JD008149.

Euskirchen, E. S., A. D. McGuire, and F. S. Chapin, 2007: Energy feedbacks of northern high-latitude ecosystems to the climate system due to reduced snow cover during 20th century warming. *Global Change Biol.*, **13**, 2425–2438, doi:10.1111/j.1365-2486.2007.01450.x.

Friedl, M. A., 2002: Forward and inverse modeling of land surface energy balance using surface temperature measurements.

Remote Sens. Environ., **79**, 344–354, doi:10.1016/S0034-4257(01)00284-X.

——, D. Sulla-Menashe, B. Tan, A. Schneider, N. Ramankutty, A. Sibley, and X. Huang, 2010: MODIS collection 5 global land cover: Algorithm refinements and characterization of new datasets. *Remote Sens. Environ.*, **114**, 168–182, doi:10.1016/j.rse.2009.08.016.

Gentine, P., D. Entekhabi, A. Chehbouni, G. Boulet, and B. Duchemin, 2007: Analysis of evaporative fraction diurnal behaviour. *Agric. For. Meteor.*, **143**, 13–29, doi:10.1016/j.agrformet.2006.11.002.

——, ——, and J. Polcher, 2011: The diurnal behavior of evaporative fraction in the soil–vegetation–atmospheric boundary layer continuum. *J. Hydrometeor.*, **12**, 1530–1546, doi:10.1175/2011JHM1261.1.

Gholz, H. L., and K. L. Clark, 2002: Energy exchange across a chronosequence of slash pine forests in Florida. *Agric. For. Meteor.*, **112**, 87–102, doi:10.1016/S0168-1923(02)00059-X.

Gilmanov, T. G., L. L. Tieszen, B. K. Wylie, L. B. Flanagan, A. B. Frank, M. R. Haferkamp, T. P. Meyers, and J. A. Morgan, 2005: Integration of CO_2 flux and remotely-sensed data for primary production and ecosystem respiration analyses in the northern Great Plains: Potential for quantitative spatial extrapolation. *Global Ecol. Biogeogr.*, **14**, 271–292, doi:10.1111/j.1466-822X.2005.00151.x.

Goulden, M. L., G. C. Winston, A. M. S. McMillan, M. E. Litvak, E. L. Read, A. V. Rocha, and J. Rob Elliot, 2006: An eddy covariance mesonet to measure the effect of forest age on land–atmosphere exchange. *Global Change Biol.*, **12**, 2146–2162, doi:10.1111/j.1365-2486.2006.01251.x.

Gu, L., and Coauthors, 2007: Influences of biomass heat and biochemical energy storages on the land surface fluxes and radiative temperature. *J. Geophys. Res.*, **112**, D02107, doi:10.1029/2006JD007425.

Gutiérrez, M. V., F. C. Meinzer, and D. A. Grantz, 1994: Regulation of transpiration in coffee hedgerows: Covariation of environmental variables and apparent responses of stomata to wind and humidity. *Plant Cell Environ.*, **17**, 1305–1313, doi:10.1111/j.1365-3040.1994.tb00532.x.

Hall, F. G., K. F. Huemmrich, S. J. Goetz, P. J. Sellers, and J. E. Nickeson, 1992: Satellite remote sensing of surface energy balance: Success, failures, and unresolved issues in FIFE. *J. Geophys. Res.*, **97**, 19 061–19 089, doi:10.1029/92JD02189.

Hardiman, B. S., G. Bohrer, C. M. Gough, C. S. Vogel, and P. S. Curtis, 2011: The role of canopy structural complexity in wood net primary production of a maturing northern deciduous forest. *Ecology*, **92**, 1818–1827, doi:10.1890/10-2192.1.

Hernandez-Ramirez, G., J. L. Hatfield, T. B. Parkin, T. J. Sauer, and J. H. Prueger, 2011: Carbon dioxide fluxes in corn–soybean rotation in the midwestern U.S.: Inter- and intra-annual variations, and biophysical controls. *Agric. For. Meteor.*, **151**, 1831–1842, doi:10.1016/j.agrformet.2011.07.017.

Hiller, R., J. McFadden, and N. Kljun, 2011: Interpreting CO_2 fluxes over a suburban lawn: The influence of traffic emissions. *Bound.-Layer Meteor.*, **138**, 215–230, doi:10.1007/s10546-010-9558-0.

Hollinger, D. Y., S. M. Goltz, E. A. Davidson, J. T. Lee, K. Tu, and H. T. Valentine, 1999: Seasonal patterns and environmental control of carbon dioxide and water vapour exchange in an ecotonal boreal forest. *Global Change Biol.*, **5**, 891–902, doi:10.1046/j.1365-2486.1999.00281.x.

——, and Coauthors, 2004: Spatial and temporal variability in forest–atmosphere CO_2 exchange. *Global Change Biol.*, **10**, 1689–1706, doi:10.1111/j.1365-2486.2004.00847.x.

——, and Coauthors, 2010: Albedo estimates for land surface models and support for a new paradigm based on foliage nitrogen concentration. *Global Change Biol.*, **16**, 696–710, doi:10.1111/j.1365-2486.2009.02028.x.

Hollinger, S. E., C. J. Bernacchi, and T. P. Meyers, 2005: Carbon budget of mature no-till ecosystem in north central region of the United States. *Agric. For. Meteor.*, **130**, 59–69, doi:10.1016/j.agrformet.2005.01.005.

Horn, J., and K. Schulz, 2010: Post-processing analysis of MODIS leaf area index subsets. *J. Appl. Remote Sens.*, **4**, 043557–043525, doi:10.1117/1.3524265.

Hu, Z., and Coauthors, 2009: Partitioning of evapotranspiration and its controls in four grassland ecosystems: Application of a two-source model. *Agric. For. Meteor.*, **149**, 1410–1420, doi:10.1016/j.agrformet.2009.03.014.

Hutyra, L. R., J. W. Munger, E. Hammond-Pyle, S. R. Saleska, N. Restrepo-Coupe, B. C. Daube, P. B. de Camargo, and S. C. Wofsy, 2008: Resolving systematic errors in estimates of net ecosystem exchange of CO_2 and ecosystem respiration in a tropical forest biome. *Agric. For. Meteor.*, **148**, 1266–1279, doi:10.1016/j.agrformet.2008.03.007.

Jastrow, J. D., R. M. Miller, and C. E. Owensby, 2000: Long-term effects of elevated atmospheric CO_2 on below-ground biomass and transformations to soil organic matter in grassland. *Plant Soil*, **224**, 85–97, doi:10.1023/A:1004771805022.

Jenkins, J. P., A. D. Richardson, B. H. Braswell, S. V. Ollinger, D. Y. Hollinger, and M. L. Smith, 2007: Refining light-use efficiency calculations for a deciduous forest canopy using simultaneous tower-based carbon flux and radiometric measurements. *Agric. For. Meteor.*, **143**, 64–79, doi:10.1016/j.agrformet.2006.11.008.

Jiang, L., S. Islam, and T. N. Carlson, 2004: Uncertainties in latent heat flux measurement and estimation: Implications for using a simplified approach with remote sensing data. *Can. J. Remote Sens.*, **30**, 769–787, doi:10.5589/m04-038.

Jung, M., M. Reichstein, and A. Bondeau, 2009: Towards global empirical upscaling of FLUXNET eddy covariance observations: Validation of a model tree ensemble approach using a biosphere model. *Biogeosciences*, **6**, 2001–2013, doi:10.5194/bg-6-2001-2009.

——, and Coauthors, 2010: Recent decline in the global land evapotranspiration trend due to limited moisture supply. *Nature*, **467**, 951–954, doi:10.1038/nature09396.

Kalma, J. D., T. R. McVicar, and M. F. McCabe, 2008: Estimating land surface evaporation: A review of methods using remotely sensed surface temperature data. *Surv. Geophys.*, **29**, 421–469, doi:10.1007/s10712-008-9037-z.

Kim, D., R. Oren, A. C. Oishi, C.-I. Hsieh, N. Phillips, K. A. Novick, and P. C. Stoy, 2014: Sensitivity of stand transpiration to wind velocity in a mixed broadleaved deciduous forest. *Agric. For. Meteor.*, **187**, 62–71, doi:10.1016/j.agrformet.2013.11.013.

Kottek, M., J. Grieser, C. Beck, B. Rudolf, and F. Rubel, 2006: World map of the Köppen-Geiger climate classification updated. *Meteor. Z.*, **15**, 259–263, doi:10.1127/0941-2948/2006/0130.

Kra, E. Y., 2010: An empirical simplification of the temperature Penman–Monteith model for the tropics. *J. Agric. Sci.*, **2**, doi:10.5539/jas.v2n1p162.

Krishnan, P., T. P. Meyers, R. L. Scott, L. Kennedy, and M. Heuer, 2012: Energy exchange and evapotranspiration over two temperate semi-arid grasslands in North America. *Agric. For. Meteor.*, **153**, 31–44, doi:10.1016/j.agrformet.2011.09.017.

Kurc, S. A., and L. M. Benton, 2010: Digital image-derived greenness links deep soil moisture to carbon uptake in a creosotebush-dominated shrubland. *J. Arid Environ.*, **74**, 585–594, doi:10.1016/j.jaridenv.2009.10.003.

Kustas, W., and M. Anderson, 2009: Advances in thermal infrared remote sensing for land surface modeling. *Agric. For. Meteor.*, **149**, 2071–2081, doi:10.1016/j.agrformet.2009.05.016.

Lei, H., Z. Zhi-Shan, and L. Xin-Rong, 2010: Sap flow of *Artemisia ordosica* and the influence of environmental factors in a re-vegetated desert area: Tengger Desert, China. *Hydrol. Processes*, **24**, 1248–1253, doi:10.1002/hyp.7584.

Lhomme, J.-P., and E. Elguero, 1999: Examination of evaporative fraction diurnal behaviour using a soil-vegetation model coupled with a mixed-layer model. *Hydrol. Earth Syst. Sci.*, **3**, 259–270, doi:10.5194/hess-3-259-1999.

Liu, H., and J. T. Randerson, 2008: Interannual variability of surface energy exchange depends on stand age in a boreal forest fire chronosequence. *J. Geophys. Res.*, **113**, G01006, doi:10.1029/2007JG000483.

Lokupitiya, E., and Coauthors, 2009: Incorporation of crop phenology in Simple Biosphere Model (SiBcrop) to improve land–atmosphere carbon exchanges from croplands. *Biogeosciences*, **6**, 969–986, doi:10.5194/bg-6-969-2009.

Luo, H., W. C. Oechel, S. J. Hastings, R. Zulueta, Y. Qian, and H. Kwon, 2007: Mature semiarid chaparral ecosystems can be a significant sink for atmospheric carbon dioxide. *Global Change Biol.*, **13**, 386–396, doi:10.1111/j.1365-2486.2006.01299.x.

Ma, S., D. D. Baldocchi, L. Xu, and T. Hehn, 2007: Inter-annual variability in carbon dioxide exchange of an oak/grass savanna and open grassland in California. *Agric. For. Meteor.*, **147**, 157–171, doi:10.1016/j.agrformet.2007.07.008.

Matamala, R., J. D. Jastrow, R. M. Miller, and C. T. Garten, 2008: Temporal changes in C and N stocks of restored prairie: Implications for C sequestration strategies. *Ecol. Appl.*, **18**, 1470–1488, doi:10.1890/07-1609.1.

Maximov, T., T. Ohta, and A. J. Dolman, 2008: Water and energy exchange in east Siberian forest: A synthesis. *Agric. For. Meteor.*, **148**, 2013–2018, doi:10.1016/j.agrformet.2008.10.004.

Meyers, T. P., and S. E. Hollinger, 2004: An assessment of storage terms in the surface energy balance of maize and soybean. *Agric. For. Meteor.*, **125**, 105–115, doi:10.1016/j.agrformet.2004.03.001.

Molotch, N. P., P. D. Brooks, S. P. Burns, M. Litvak, R. K. Monson, J. R. McConnell, and K. Musselman, 2009: Ecohydrological controls on snowmelt partitioning in mixed-conifer sub-alpine forests. *Ecohydrology*, **2**, 129–142, doi:10.1002/eco.48.

Monteith, J., 1965: Evaporation and environment. *Symp. Soc. Exp. Biol.*, **19**, 205–224.

Montgomery, D. C., E. A. Peck, and G. G. Vining, 2012: *Introduction to Linear Regression Analysis.* John Wiley and Sons, 672 pp.

Mu, Q., F. A. Heinsch, M. Zhao, and S. W. Running, 2007a: Development of a global evapotranspiration algorithm based on MODIS and global meteorology data. *Remote Sens. Environ.*, **111**, 519–536, doi:10.1016/j.rse.2007.04.015.

——, M. S. Zhao, F. A. Heinsch, M. L. Liu, H. Q. Tian, and S. W. Running, 2007b: Evaluating water stress controls on primary production in biogeochemical and remote sensing based models. *J Geophys Res.*, **112**, G01012, doi:10.1029/2006JG000179.

——, ——, and S. W. Running, 2011: Improvements to a MODIS global terrestrial evapotranspiration algorithm. *Remote Sens. Environ.*, **115**, 1781–1800, doi:10.1016/j.rse.2011.02.019.

Muldavin, E., D. Moore, S. Collins, K. Wetherill, and D. Lightfoot, 2008: Aboveground net primary production dynamics in a northern Chihuahuan Desert ecosystem. *Oecologia*, **155**, 123–132, doi:10.1007/s00442-007-0880-2.

Nichols, W. E., and R. H. Cuenca, 1993: Evaluation of the evaporative fraction for parameterization of the surface energy balance. *Water Resour. Res.*, **29**, 3681–3690, doi:10.1029/93WR01958.

Norman, J. M., W. P. Kustas, J. H. Prueger, and G. R. Diak, 2000: Surface flux estimation using radiometric temperature: A dual temperature-difference method to minimize measurement errors. *Water Resour. Res.*, **36**, 2263–2274, doi:10.1029/2000WR900033.

Peng, J., M. Borsche, Y. Liu, and A. Loew, 2013: How representative are instantaneous evaporative fraction measurements of daytime fluxes? *Hydrol. Earth Syst. Sci.*, **17**, 3913–3919, doi:10.5194/hess-17-3913-2013.

Powell, T. L., H. L. Gholz, K. L. Clark, G. Starr, W. P. Cropper, and T. A. Martin, 2008: Carbon exchange of a mature, naturally regenerated pine forest in north Florida. *Global Change Biol.*, **14**, 2523–2538, doi:10.1111/j.1365-2486.2008.01675.x.

Priestley, C., and R. Taylor, 1972: On the assessment of surface heat flux and evaporation using large-scale parameters. *Mon. Wea. Rev.*, **100**, 81–92, doi:10.1175/1520-0493(1972)100<0081:OTAOSH>2.3.CO;2.

Ricciuto, D. M., M. P. Butler, K. J. Davis, B. D. Cook, P. S. Bakwin, A. Andrews, and R. M. Teclaw, 2008: Causes of interannual variability in ecosystem–atmosphere CO_2 exchange in a northern Wisconsin forest using a Bayesian model calibration. *Agric. For. Meteor.*, **148**, 309–327, doi:10.1016/j.agrformet.2007.08.007.

Rivas, R., and V. Caselles, 2004: A simplified equation to estimate spatial reference evaporation from remote sensing-based surface temperature and local meteorological data. *Remote Sens. Environ.*, **93**, 68–76, doi:10.1016/j.rse.2004.06.021.

Román, M. O., and Coauthors, 2009: The MODIS (collection V005) BRDF/albedo product: Assessment of spatial representativeness over forested landscapes. *Remote Sens. Environ.*, **113**, 2476–2498, doi:10.1016/j.rse.2009.07.009.

Saugier, B., A. Granier, J. Y. Pontailler, E. Dufrêne, and D. D. Baldocchi, 1997: Transpiration of a boreal pine forest measured by branch bag, sap flow and micrometeorological methods. *Tree Physiol.*, **17**, 511–519, doi:10.1093/treephys/17.8-9.511.

Schmidt, A., C. Hanson, J. Kathilankal, and B. E. Law, 2011: Classification and assessment of turbulent fluxes above ecosystems in North-America with self-organizing feature map networks. *Agric. For. Meteor.*, **151**, 508–520, doi:10.1016/j.agrformet.2010.12.009.

Scott, R. L., 2010: Using watershed water balance to evaluate the accuracy of eddy covariance evaporation measurements for three semiarid ecosystems. *Agric. For. Meteor.*, **150**, 219–225, doi:10.1016/j.agrformet.2009.11.002.

Shaw, D., J. Franklin, K. Bible, J. Klopatek, E. Freeman, S. Greene, and G. Parker, 2004: Ecological setting of the Wind River old-growth forest. *Ecosystems*, **7**, 427–439, doi:10.1007/s10021-004-0135-6.

Shuttleworth, W. J., 1991: Insight from large-scale observational studies of land/atmosphere interactions. *Surv. Geophys.*, **12**, 3–30, doi:10.1007/BF01903410.

——, 2007: Putting the ''vap'' into evaporation. *Hydrol. Earth Syst. Sci.*, **11**, 210–244, doi:10.5194/hess-11-210-2007.

Si, J.-H., Q. Feng, X.-Y. Zhang, Z.-Q. Chang, Y.-H. Su, and H.-Y. Xi, 2007: Sap flow of *Populus euphratica* in a desert

riparian forest in an extreme arid region during the growing season. *J. Integr. Plant Biol.*, **49**, 425–436, doi:10.1111/j.1744-7909.2007.00388.x.

Smith, E. A., and Coauthors, 1992: Area-averaged surface fluxes and their time-space variability over the FIFE experimental domain. *J. Geophys. Res.*, **97**, 18 599–18 622, doi:10.1029/91JD03060.

Stoy, P. C., G. G. Katul, M. B. S. Siqueira, J.-Y. Juang, H. R. McCarthy, H.-S. Kim, A. C. Oishi, and R. Oren, 2005: Variability in net ecosystem exchange from hourly to inter-annual time scales at adjacent pine and hardwood forests: A wavelet analysis. *Tree Physiol.*, **25**, 887–902, doi:10.1093/treephys/25.7.887.

Sulman, B., A. Desai, B. Cook, N. Saliendra, and D. Mackay, 2009: Contrasting carbon dioxide fluxes between a drying shrub wetland in northern Wisconsin, USA, and nearby forests. *Biogeosciences*, **6**, 1115–1126, doi:10.5194/bg-6-1115-2009.

Tanaka, N., and Coauthors, 2008: A review of evapotranspiration estimates from tropical forests in Thailand and adjacent regions. *Agric. For. Meteor.*, **148**, 807–819, doi:10.1016/j.agrformet.2008.01.011.

Teixeira, A. H. D. C., W. G. M. Bastiaanssen, M. D. Ahmad, and M. G. Bos, 2009a: Reviewing SEBAL input parameters for assessing evapotranspiration and water productivity for the low-middle São Francisco River basin, Brazil: Part A: Calibration and validation. *Agric. For. Meteor.*, **149**, 462–476, doi:10.1016/j.agrformet.2008.09.016.

——, ——, ——, and ——, 2009b: Reviewing SEBAL input parameters for assessing evapotranspiration and water productivity for the low-middle São Francisco River basin, Brazil: Part B: Application to the regional scale. *Agric. For. Meteor.*, **149**, 477–490, doi:10.1016/j.agrformet.2008.09.014.

Timmermans, W. J., W. P. Kustas, M. C. Anderson, and A. N. French, 2007: An intercomparison of the surface energy balance algorithm for land (SEBAL) and the two-source energy balance (TSEB) modeling schemes. *Remote Sens. Environ.*, **108**, 369–384, doi:10.1016/j.rse.2006.11.028.

Twine, T. E., and Coauthors, 2000: Correcting eddy-covariance flux underestimates over a grassland. *Agric. For. Meteor.*, **103**, 279–300, doi:10.1016/S0168-1923(00)00123-4.

Urbanski, S., and Coauthors, 2007: Factors controlling CO_2 exchange on timescales from hourly to decadal at Harvard Forest. *J. Geophys. Res.*, **112**, G02020, doi:10.1029/2006JG000293.

Valiantzas, J. D., 2006: Simplified versions for the Penman evaporation equation using routine weather data. *J. Hydrol.*, **331**, 690–702, doi:10.1016/j.jhydrol.2006.06.012.

——, 2013: Simplified forms for the standardized FAO-56 Penman–Monteith reference evapotranspiration using limited weather data. *J. Hydrol.*, **505**, 13–23, doi:10.1016/j.jhydrol.2013.09.005.

van Gorsel, E., and Coauthors, 2009: Estimating nocturnal ecosystem respiration from the vertical turbulent flux and change in storage of CO_2. *Agric. For. Meteor.*, **149**, 1919–1930, doi:10.1016/j.agrformet.2009.06.020.

Verma, S. B., and Coauthors, 2005: Annual carbon dioxide exchange in irrigated and rainfed maize-based agroecosystems. *Agric. For. Meteor.*, **131**, 77–96, doi:10.1016/j.agrformet.2005.05.003.

Wang, K., 2014: Sampling biases in datasets of historical mean air temperature over land. *Sci. Rep.*, **4**, 4637, doi:10.1038/srep04637.

——, and S. Liang, 2008: An improved method for estimating global evapotranspiration based on satellite determination of surface net radiation, vegetation index, temperature, and soil moisture. *J. Hydrometeor.*, **9**, 712–727, doi:10.1175/2007JHM911.1.

——, and ——, 2009: Estimation of daytime net radiation from shortwave radiation measurements and meteorological observations. *J. Appl. Meteor. Climatol.*, **48**, 634–643, doi:10.1175/2008JAMC1959.1.

——, and R. E. Dickinson, 2012: A review of global terrestrial evapotranspiration: Observation, modeling, climatology, and climatic variability. *Rev. Geophys.*, **50**, RG2005, doi:10.1029/2011RG000373.

——, and C. Zhou, 2015: Regional contrasts of the warming rate over land significantly depend on the calculation methods of mean air temperature. *Sci. Rep.*, **5**, 12324, doi:10.1038/srep12324.

——, Z. Li, and M. Cribb, 2006: Estimation of evaporative fraction from a combination of day and night land surface temperatures and NDVI: A new method to determine the Priestley–Taylor parameter. *Remote Sens. Environ.*, **102**, 293–305, doi:10.1016/j.rse.2006.02.007.

——, P. Wang, Z. Li, M. Cribb, and M. Sparrow, 2007: A simple method to estimate actual evapotranspiration from a combination of net radiation, vegetation index, and temperature. *J. Geophys. Res.*, **112**, D15107, doi:10.1029/2006JD008351.

——, R. E. Dickinson, and S. Liang, 2008: Observational evidence on the effects of clouds and aerosols on net ecosystem exchange and evapotranspiration. *Geophys. Res. Lett.*, **35**, L10401, doi:10.1029/2008GL034167.

——, ——, M. Wild, and S. Liang, 2010: Evidence for decadal variation in global terrestrial evapotranspiration between 1982 and 2002: 1. Model development. *J. Geophys. Res.*, **115**, D20112, doi:10.1029/2009JD013671.

Wilson, K., and Coauthors, 2002: Energy balance closure at FLUXNET sites. *Agric. For. Meteor.*, **113**, 223–243, doi:10.1016/S0168-1923(02)00109-0.

Wilson, T. B., and T. P. Meyers, 2007: Determining vegetation indices from solar and photosynthetically active radiation fluxes. *Agric. For. Meteor.*, **144**, 160–179, doi:10.1016/j.agrformet.2007.04.001.

Xiao, J., and Coauthors, 2008: Estimation of net ecosystem carbon exchange for the conterminous United States by combining MODIS and AmeriFlux data. *Agric. For. Meteor.*, **148**, 1827–1847, doi:10.1016/j.agrformet.2008.06.015.

Zahumenský, I., 2004: Guidelines on quality control procedures for data from automatic weather stations. World Meteorological Organization Proposal CIMO/OPAG-SURFACE/ ET ST&MT-1/Doc.6.1(2), 10 pp. [Available online at www.wmo.int/pages/prog/www/IMOP/meetings/Surface/ET-STMT1_Geneva2004/Doc6.1(2).pdf.]

Zha, T., A. G. Barr, G. van der Kamp, T. A. Black, J. H. McCaughey, and L. B. Flanagan, 2010: Interannual variation of evapotranspiration from forest and grassland ecosystems in western Canada in relation to drought. *Agric. For. Meteor.*, **150**, 1476–1484, doi:10.1016/j.agrformet.2010.08.003.